Gd-doped $BaSnO_3$: A transparent conducting oxide with localized magnetic moments

Urusa S. Alaan, Padraic Shafer, Alpha T. N'Diaye, Elke Arenholz, and Y. Suzuki

Citation: Appl. Phys. Lett. **108**, 042106 (2016); doi: 10.1063/1.4939686
View online: https://doi.org/10.1063/1.4939686
View Table of Contents: http://aip.scitation.org/toc/apl/108/4
Published by the American Institute of Physics

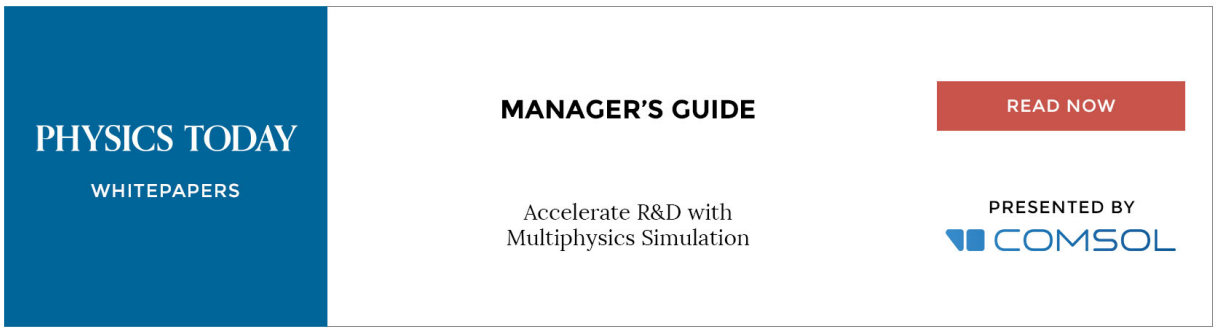

Gd-doped $BaSnO_3$: A transparent conducting oxide with localized magnetic moments

Urusa S. Alaan,[1,2,a)] Padraic Shafer,[3] Alpha T. N'Diaye,[3] Elke Arenholz,[3] and Y. Suzuki[2,4]
[1]*Department of Materials Science and Engineering, Stanford University, Stanford, California 94305, USA*
[2]*Geballe Laboratory for Advanced Materials, Stanford University, Stanford, California 94305, USA*
[3]*Advanced Light Source, Lawrence Berkeley National Laboratory, Berkeley, California 94720, USA*
[4]*Department of Applied Physics, Stanford University, Stanford, California 94305, USA*

(Received 17 October 2015; accepted 27 December 2015; published online 28 January 2016)

We have synthesized transparent, conducting, paramagnetic stannate thin films via rare-earth doping of $BaSnO_3$. Gd^{3+} ($4f^7$) substitution on the Ba^{2+} site results in optical transparency in the visible regime, low resistivities, and high electron mobilities, along with a significant magnetic moment. Pulsed laser deposition was used to stabilize epitaxial $Ba_{0.96}Gd_{0.04}SnO_3$ thin films on (001) $SrTiO_3$ substrates, and compared with $Ba_{0.96}La_{0.04}SnO_3$ and undoped $BaSnO_3$ thin films. Gd as well as La doping schemes result in electron mobilities at room temperature that exceed those of conventional complex oxides, with values as high as $60\,cm^2/V{\cdot}s$ ($n = 2.5 \times 10^{20}\,cm^{-3}$) and $30\,cm^2/V{\cdot}s$ ($n = 1 \times 10^{20}\,cm^{-3}$) for La and Gd doping, respectively. The resistivity shows little temperature dependence across a broad temperature range, indicating that in both types of films the transport is not dominated by phonon scattering. Gd-doped $BaSnO_3$ films have a strong magnetic moment of $\sim 7\ \mu_B$/Gd ion. Such an optically transparent conductor with localized magnetic moments may unlock opportunities for multifunctional devices in the design of next-generation displays and photovoltaics. © *2016 AIP Publishing LLC*. [http://dx.doi.org/10.1063/1.4939686]

Spin-based electronics, or "spintronics," is an emerging technology that could offer faster devices with low power requirements through simultaneous control of both the spin and charge degrees of freedom in a materials system. Where conventional charge-based devices rely only on the motion of the charge of an electron, the ability of semiconductor spintronic devices to utilize the electron spin component additionally allows for nonvolatility and higher integration densities.[1] If optical transparency is achieved in a ferromagnetic semiconductor, it will unlock opportunities for multifunctional opto-magnetoelectric devices in the design of next-generation displays and photovoltaics.[2,3]

One route to achieving a transparent conductor is through doping of the perovskite structure $BaSnO_3$. It has been recently shown that when $BaSnO_3$ is doped with La on the Ba-site, the result is a high-mobility transparent conducting oxide (TCO).[4–6] In bulk crystals, mobilities as high as $300\,cm^2/V{\cdot}s$ at room temperature have been realized, while in thin films the highest reported electron mobilities are $\sim 100\,cm^2/V{\cdot}s$ and seemingly suppressed due to threading dislocations.[4,6,7] Even in the thin film cases, such high mobilities at room temperature combined with optical transparency in a perovskite structure make $BaSnO_3$ an attractive candidate for creating a dilute magnetic conductor for opto-magntoelectronic devices.

Recent studies have shown that magnetic dopants such as various 3*d* transition metals (Mn, Fe, and Co) can be incorporated onto the Sn^{4+} site of $BaSnO_3$.[8–11] With these 3*d* transition metal dopants, some studies have reported a ferromagnetic signal in $BaSnO_3$, though the resulting samples are insulating and opaque in the visible wavelength range. If the ferromagnetism is intrinsic, it is hypothesized to result from an "F-center exchange" mechanism, which relies on oxygen vacancies that trap electrons and cause local ferromagnetic ordering. However, the need for charge carriers to be localized and strongly coupled to defect sites impedes their conduction. Efforts to co-dope $BaSnO_3$ with two transition metals on the Sn site to add both conduction and a magnetic moment have also resulted in insulating materials.[12]

For this reason, we have chosen to develop magnetic functionality through A-site doping with a magnetic rare-earth element. If Gd^{3+} ($4f^7$) substitutes for Ba^{2+} on the A-site, we have an aliovalent doping scheme and the introduction of both charge and a magnetic moment with a single dopant. In this study, we show that $Ba_{1-x}Gd_xSnO_3$ films are transparent, conducting, and also paramagnetic.

We have synthesized $Ba_{0.96}La_{0.04}SnO_3$ (La:BSO or BLSO), $Ba_{0.96}Gd_{0.04}SnO_3$ (Gd:BSO or BGSO), and undoped $BaSnO_3$ (BSO) thin films by pulsed laser deposition on (001) $SrTiO_3$ substrates. All films were grown at 750 °C and 100 mTorr O_2 with a laser fluence of $\sim 1.4\,J/cm^2$ ($\lambda = 248$ nm). A Quantum Design Physical Property Measurement System and Magnetic Property Measurement System (SQUID magnetometer) were used to ascertain electronic transport and magnetization data, respectively. X-ray absorption spectroscopy (XAS) and x-ray magnetic circular dichroism (XMCD) measurements were conducted in total electron yield mode at Beamlines 4.0.2 and 6.3.1 of the Advanced Light Source. Rutherford backscattering spectrometry (RBS) in the Cornell geometry with a NEC model 5SDH Pelletron tandem accelerator and helium source was used to obtain film thicknesses and stoichiometries.

Both the Gd- and La-doped $BaSnO_3$ films are transparent and colorless in the visible spectrum. Figure 1 shows

a)Author to whom correspondence should be addressed. Electronic mail: usalaan@gmail.com

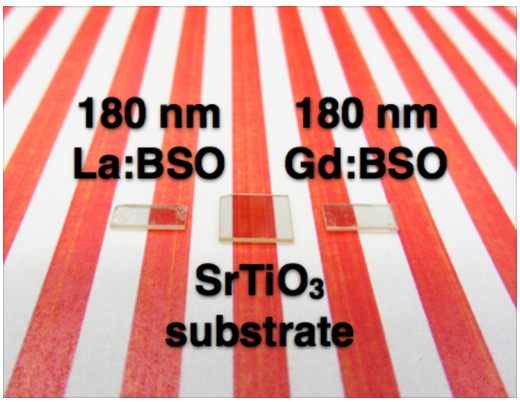

FIG. 1. La-doped and Gd-doped $BaSnO_3$ films are colorless and transparent. A (001) $SrTiO_3$ substrate is shown for comparison.

180 nm thick films on (001) $SrTiO_3$ substrates along with a bare substrate for comparison. Using RBS (not shown) and XAS (cf. Figure 5(a) for Gd:BSO), we verified that both Gd and La were incorporated into the films. Although the nominal doping concentration of both La and Gd in the targets was 4%, the measured RBS stoichiometry gave ~7% La doping for La:BSO films and ~5% doping for Gd:BSO films in this study.

Despite the large lattice mismatch of ~5% between $BaSnO_3$ (a = 4.098 Å) and $SrTiO_3$ (a = 3.905 Å), $BaSnO_3$ films grow epitaxially on $SrTiO_3$. Figure 2(a) shows out-of-plane x-ray diffraction scans with {001} film reflections, corresponding to the associated substrate Bragg peaks. Azithumal ϕ scans of the 110 peak in Figure 2(b) demonstrate in-plane alignment of the film and substrate, confirming an epitaxial relationship. Gd:BSO films have an out-of-plane lattice parameter of $a = 4.122$ Å, and La:BSO films have $a = 4.134$ Å, as calculated from the 002 reflection. The undoped film, shown for comparison, has an out-of-plane lattice parameter of $a = 4.124$ Å. All films are fully relaxed, as measured by reciprocal space mapping. The lattice parameter of La:BSO increases from the undoped BSO case even though the ionic radius of La^{3+} (1.36 Å) is 16% smaller than that of Ba^{2+} (1.61 Å).[13,14] Lattice expansion as a result of electron doping is expected and is attributed to the presence of antibonding states in the conduction band.[6,15] Doping with Gd^{3+}, for which the extrapolated ionic radius with a coordination of 12 is ~1.28 Å, is even smaller than La^{3+} and yet does not change the lattice constant of BSO from the undoped case.[13,14] Therefore, the expected contraction of the lattice due to a smaller cation may be counteracted by electron doping.[6,15–17] The full-width-at-half-maximum of the rocking curves, an indicator of the crystalline quality and mosaic spread of the films, is $\Delta\omega_{002} = 0.040°$ for Gd:BSO and $\Delta\omega_{002} = 0.087°$ for La:BSO. Therefore, despite the introduction of a dopant with a larger radius difference with Ba, these Gd:BSO films actually may have fewer dislocations than the La:BSO films.

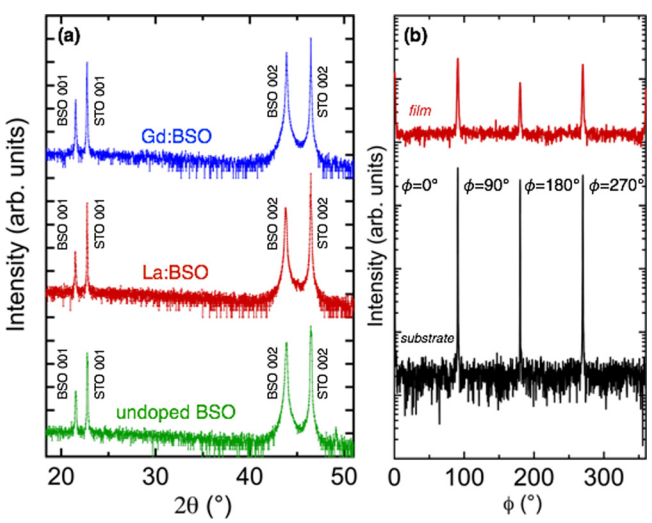

FIG. 2. (a) X-ray diffraction θ-2θ scans show that the films are ordered and textured, and (b) ϕ-scans of the 110 peak confirm epitaxy of (001)-oriented $BaSnO_3$ on (001)-oriented $SrTiO_3$.

Electrical transport measurements for the doped films indicate metallic behavior (Figure 3). The undoped films are insulating, as predicted theoretically and shown experimentally by other groups.[18,19] Gd-doping of BSO results in n-type metallic conduction, with minimal temperature dependence from 2 to 380 K. At 300 K, the Gd:BSO films have resistivities of $\rho \sim 2$ mΩ·cm, mobilities of $\mu_e \sim 28\ cm^2/V{\cdot}s$, and carrier concentrations of approximately $n = 1.0 \times 10^{20}\ cm^{-3}$. At lower temperatures, there is little change in the transport properties, with $\mu_e \sim 35\ cm^2/V{\cdot}s$ at 2 K. For La:BSO, the room-temperature values are $\rho \sim 0.4$ mΩ·cm, $\mu_e \sim 58\ cm^2/V{\cdot}s$, and $n = 2.5 \times 10^{20}\ cm^{-3}$. Again, the films are metallic with little change at 2 K ($\rho \sim 0.3$ mΩ·cm, $\mu_e \sim 82\ cm^2/V{\cdot}s$). The lack of a temperature dependence indicates that phonons are not the dominant scattering mechanism in either Gd:BSO or La:BSO, and instead defects may play a significant role. The electron

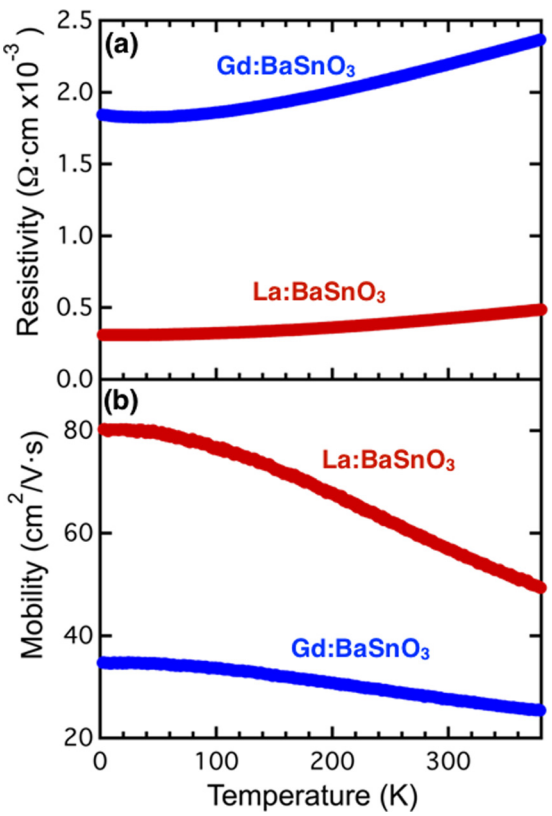

FIG. 3. (a) van der Pauw resistivity and (b) electron mobilities across the temperature range of 2–380 K.

mobilities for both La- and Gd-doped films are significantly higher than those of typical complex oxides at room temperature, for which μ_e is usually $<10\,cm^2/V{\cdot}s$.[6,7,20–26] The mobilities of our La-doped thin films are comparable to those measured by other groups on $Ba_{0.96}La_{0.04}SnO_3$ thin films, for which the highest reported room-temperature mobility is $\sim 66\,cm^2/V{\cdot}s$.[5,6,27–30] Our Gd-doped BSO films have mobilities and carrier concentrations lower than those of our La-doped BSO films. This observation can be explained by considering local strain fields surrounding the dopant atom in its host environment. If the substitutional cation is more dissimilar in size to the equilibrium site occupancy, it follows that the lattice will be more *locally* distorted than the case with a dopant that is more similar in size. Since Gd^{3+} has a greater size mismatch with Ba^{2+} than La^{3+} does, these local distortions in the strain field around the dopant atom may be more pronounced and lead to suppressed mobilities. Furthermore, the introduction of magnetic impurities may lead to additional scattering that further reduces electron mobilities.[31,32]

SQUID magnetometry revealed that Gd-doping of $BaSnO_3$ results in a large paramagnetic moment. The magnetization response of a 2.5 μm thick $Ba_{0.96}Gd_{0.04}SnO_3$ film to an applied field at 4.5 K after field-cooling in +7 T is given in Figure 4. The large magnetic moment is linear at low fields, but becomes non-linear around 1 T. By 7 T, the magnetization appears to saturate at 45 emu/cm^3. The shape of the magnetic response is described accurately by a Brillouin function with $g = 2$ and $J = 7/2$ for Gd, shown by the green line in Figure 4. At 7 T, the saturation magnetization corresponds to $\sim 7\,\mu_B$/Gd^{3+}—the full spin moment expected from Gd 4f shell—within experimental error. A closer inspection of the magnetization loop reveals that there is no apparent hysteresis within the resolution of the SQUID magnetometer. The temperature-dependent magnetization is well-fit by Curie's law, which is consistent with a paramagnetic ground state.

We used XAS and XMCD to probe the absorption edge of Gd and confirm the origin of the magnetic moment. These experiments were performed in total electron yield mode with a probing depth of ~5 nm and an angle of x-ray incidence at 30° grazing to the sample surface. In Figure 5, we show the

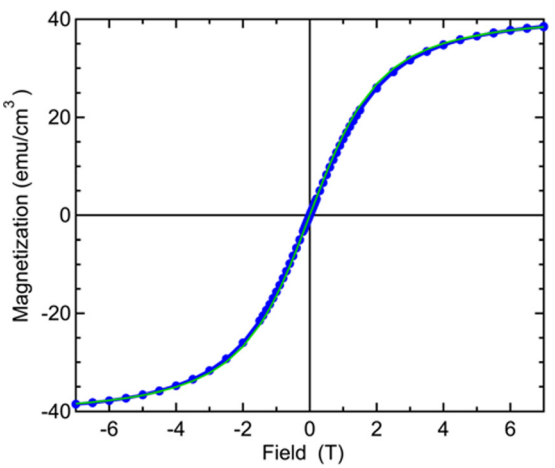

FIG. 4. A magnetization versus field loop of a Gd-doped $BaSnO_3$, as measured by SQUID magnetometry. The green line is the Brillouin function for Gd, normalized to the magnetization.

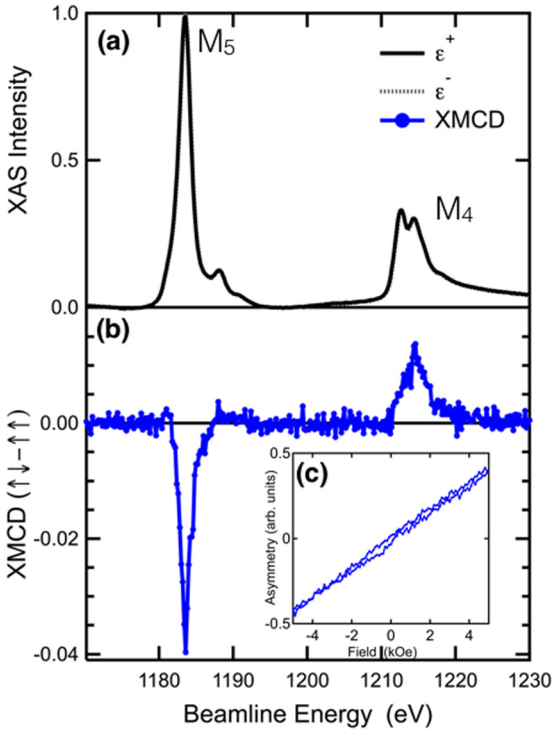

FIG. 5. (a) X-ray absorption (XAS) spectra (with opposite circular polarizations ε^+ and ε^-) of the Gd M_5 and M_4 edges at 15 K confirm Gd incorporation into the $BaSnO_3$ films, and the (b) difference between these XAS measurements with ε^+ and ε^- gives a clear XMCD signal. (c) Magnetic asymmetry versus field measurements in the range $H = \pm 0.5$ T are linear and non-hysteretic, consistent with a paramagnetic response.

Gd $M_{5,4}$ edges of Gd:BSO. There is a clear XMCD signal that follows the lineshape expected for Gd, thereby confirming that Gd dopants are the origin of the observed magnetometry result.[33] Figure 5(c) shows the XMCD asymmetry as function of applied magnetic field between ±0.5 T. The loops show no hysteresis, further indicating that Gd:BSO is paramagnetic.

Together the bulk magnetometry measurements and XMCD measurements suggest that there is no long-range magnetic order in the Gd-doped samples. One avenue toward ferromagnetism in such systems could be to increase the doping level of Gd in BSO, thereby increasing the number of delocalized carriers to mediate a Ruderman-Kittel-Kasuya-Yosida-type interaction. Therefore, while it may be favorable for electronic transport to dope with lower concentrations in order to achieve higher mobility values, the conductivity and magnetic response are enhanced by raising the Gd doping levels. The doping level of Gd thus provides the ability to tune the functional properties of Gd:$BaSnO_3$ to match the requirements of the desired application.

In summary, we have synthesized Gd-doped $BaSnO_3$ and shown that Gd can be incorporated into BSO. The result is a good transparent conducting oxide, with high room-temperature electron mobility values. The addition of a magnetic moment while preserving metallicity as well as optical transparency can be useful in the fabrication of functional devices, with the ability to further tailor functionality via the Gd concentration.

We thank Dr. Franklin J. Wong for his ideas and insight. We also thank Dr. Useong Kim and Professor Kookrin Char

for their advice on the growth of $BaSnO_3$. We are grateful for useful discussions with Matthew T. Gray, Charles L. Flint, Ted D. Sanders, Purnima Parvathy Balakrishnan, and Michael J. Veit. The research was funded by the Army Research Office under Grant No. W911NF-14-1-0611. U.S.A. was supported in part by the National Science Foundation Graduate Research Fellowship Program. The Advanced Light Source is supported by the Director, Office of Science, Office of Basic Energy Sciences, of the U.S. Department of Energy under Contract No. DE-AC02-05CH11231. All x-ray diffraction measurements in this work were conducted at the Stanford Nano Shared Facilities (SNSF).

[1]S. A. Wolf, D. D. Awschalom, R. A. Buhrman, J. M. Daughton, S. von Molnár, M. L. Roukes, A. Y. Chtchelkanova, and D. M. Treger, Science **294**, 1488 (2001).
[2]J. Philip, A. Punnoose, B. I. Kim, K. M. Reddy, S. Layne, J. O. Holmes, B. Satpati, P. R. Leclair, T. S. Santos, and J. S. Moodera, Nat. Mater. **5**, 298 (2006).
[3]K. Sato and H. Katayama-Yoshida, Semicond. Sci. Technol. **17**, 367 (2002).
[4]X. Luo, Y. S. Oh, A. Sirenko, P. Gao, T. A. Tyson, K. Char, and S.-W. Cheong, Appl. Phys. Lett. **100**, 172112 (2012).
[5]H. J. Kim, U. Kim, H. M. Kim, T. H. Kim, H. S. Mun, B.-G. Jeon, K. T. Hong, W.-J. Lee, C. Ju, K. H. Kim, and K. Char, Appl. Phys. Express **5**, 061102 (2012).
[6]H. J. Kim, U. Kim, T. H. Kim, J. Kim, H. M. Kim, B.-G. Jeon, W.-J. Lee, H. S. Mun, K. T. Hong, J. Yu, K. Char, and K. H. Kim, Phys. Rev. B **86**, 165205 (2012).
[7]S. Ismail-Beigi, F. J. Walker, S.-W. Cheong, K. M. Rabe, and C. H. Ahn, APL Mater. **3**, 062510 (2015).
[8]K. Balamurugan, N. H. Kumar, J. A. Chelvane, and P. N. Santhosh, J. Alloys Compd. **472**, 9 (2009).
[9]Q. Liu, Y. He, H. Li, B. Li, G. Gao, L. Fan, and J. Dai, Appl. Phys. Express **7**, 033006 (2014).
[10]K. K. James, A. Aravind, and M. K. Jayaraj, Appl. Surf. Sci. **282**, 121 (2013).
[11]O. Parkash, D. Kumar, K. K. Srivastav, and R. K. Dwivedi, J. Mater. Sci. **36**, 5805 (2001).
[12]K. Balamurugan, N. Harish Kumar, J. Arout Chelvane, and P. N. Santhosh, Phys. B: Condens. Matter **407**, 2519 (2012).
[13]R. D. Shannon and C. T. Prewitt, Acta Crystallogr., Sect. B: Struct. Crystallogr. Cryst. Chem. **25**, 925 (1969).
[14]R. D. Shannon, Acta Crystallogr., Sect. A **32**, 751 (1976).
[15]M. Leszczyński, E. Litwin-Staszewska, and T. Suski, Acta Phys. Pol., A **88**, 837 (1995).
[16]E. R. Vance, R. A. Day, Z. Zhang, B. D. Begg, C. J. Ball, and M. G. Blackford, J. Solid State Chem. **124**, 77 (1996).
[17]Y. Sakaki, Y. Takeda, A. Kato, N. Imanishi, O. Yamamoto, M. Hattori, M. Iio, and Y. Esaki, Solid State Ionics **118**, 187 (1999).
[18]T. N. Stanislavchuk, A. A. Sirenko, A. P. Litvinchuk, X. Luo, and S.-W. Cheong, J. Appl. Phys. **112**, 044108 (2012).
[19]D. O. Scanlon, Phys. Rev. B **87**, 161201 (2013).
[20]O. N. Tufte and P. W. Chapman, Phys. Rev. **155**, 796 (1967).
[21]K. Ueda, H. Yanagi, H. Hosono, and H. Kawazoe, Phys. Rev. B **56**, 12998 (1997).
[22]T. Okuda, K. Nakanishi, S. Miyasaka, and Y. Tokura, Phys. Rev. B **63**, 113104 (2001).
[23]T. Kolodiazhnyi, A. Petric, M. Niewczas, C. Bridges, A. Safa-Sefat, and J. E. Greedan, Phys. Rev. B **68**, 085205 (2003).
[24]J. Son, P. Moetakef, B. Jalan, O. Bierwagen, N. J. Wright, R. Engel-Herbert, and S. Stemmer, Nat. Mater. **9**, 482 (2010).
[25]R. Martínez, A. Kumar, R. Palai, R. S. Katiyar, and J. F. Scott, J. Appl. Phys. **107**, 114107 (2010).
[26]C. Park, U. Kim, C. J. Ju, J. S. Park, Y. M. Kim, and K. Char, Appl. Phys. Lett. **105**, 203503 (2014).
[27]H. F. Wang, Q. Z. Liu, F. Chen, G. Y. Gao, W. Wu, and X. H. Chen, J. Appl. Phys. **101**, 106105 (2007).
[28]S. Sallis, D. O. Scanlon, S. C. Chae, N. F. Quackenbush, D. A. Fischer, J. C. Woicik, J.-H. Guo, S.-W. Cheong, and L. F. J. Piper, Appl. Phys. Lett. **103**, 042105 (2013).
[29]H. Mun, U. Kim, H. Min Kim, C. Park, T. Hoon Kim, H. Joon Kim, K. Hoon Kim, and K. Char, Appl. Phys. Lett. **102**, 252105 (2013).
[30]U. Kim, C. Park, T. Ha, R. Kim, H. S. Mun, H. M. Kim, H. J. Kim, T. H. Kim, N. Kim, J. Yu, K. H. Kim, J. H. Kim, and K. Char, APL Mater. **2**, 056107 (2014).
[31]J. Kossut, Phys. Status Solidi **72**, 359 (1975).
[32]J. Kossut, Phys. Status Solidi **78**, 537 (1976).
[33]J. Stöhr and H. C. Siegmann, *Magnetism: From Fundamentals to Nanoscale Dynamics* (Springer, 2006).